

so that

$$u_x(k,0) = p_{ix0}' e^{ikx_{i0}'} / \rho A_x. \quad (\text{A2.6})$$

The initial pressure condition turns out to be immaterial for the final result and a reasonable choice is

$$\mathfrak{P}(k,0) = 0, \quad (\text{A2.7})$$

corresponding to uniform pressure initially. The solution of Eq. (A2.1) is

$$\mathfrak{Z} = \exp(\mathbf{M}t) \mathfrak{Z}_0. \quad (\text{A2.8})$$

It is easily shown that the second moment is related to the Fourier transform by

$$\begin{aligned} M^{(\psi)} &= \int_{-\infty}^{\infty} (x - x_{i0})^2 u_x(x,t) dx \\ &= -\frac{\partial^2}{\partial k^2} [u_x(k,t) e^{-ikx_{i0}'}]_{k=0}. \end{aligned} \quad (\text{A2.9})$$

One finds that

$$\begin{aligned} &\int_{-\infty}^{\infty} (x - x_{i0}')^2 Z(x,t) dx \\ &= -\frac{\partial^2}{\partial k^2} [\mathfrak{Z}(k,t) e^{-ikx_{i0}'}]_{k=0}, \end{aligned} \quad (\text{A2.10})$$

$$= -\left[ t \frac{\partial^2 \mathbf{M}}{\partial^2 k} + t^2 \left( \frac{\partial \mathbf{M}}{\partial k} \right)^2 \right]_{k=0} (\mathfrak{Z}_0 e^{-ikx_{i0}'}), \quad (\text{A2.11})$$

$$= \left[ t \begin{pmatrix} 2\psi/\rho & 0 \\ 0 & 0 \end{pmatrix} + t^2 \begin{pmatrix} c_s^2 & 0 \\ 0 & c_s^2 \end{pmatrix} \right] \begin{pmatrix} p_{ix0}' / \rho A_x \\ 0 \end{pmatrix}, \quad (\text{A2.12})$$

from which Eq. (4.7) follows.

### APPENDIX III

By conservation of a pressure fluctuation we mean that the integral of the instantaneous pressure over all space is independent of time. To show that Eqs. (4.1) and (4.6) imply this result we must examine

$$\int_{-\infty}^{\infty} P(x,t) dx = \mathfrak{P}(0,t). \quad (\text{A3.1})$$

The matrix  $\mathbf{M}$  is zero for  $k=0$  so that Eq. (A2.8) expresses the conservation condition in the form  $\mathfrak{P}(0,t) = \mathfrak{P}(0,0)$ . (We are no longer assuming that at zero time there are no pressure fluctuations.)

## Effect of the $\lambda$ Transition on the Atomic Distribution in Liquid Helium by Neutron Diffraction

D. G. HENSHAW

*Division of Physics, Atomic Energy of Canada Limited, Chalk River, Ontario, Canada*

(Received January 18, 1960)

Neutron diffraction patterns for samples of liquid helium at 1.06°K, 2.29°K, and 2.46°K have been measured over the angular range 4° to 64° using 1.064 Å neutrons. The liquid structure factor  $i(s)+1$  is deduced for each curve and these show a change which is associated with the  $\lambda$  transition which indicates that the spatial order in the liquid is smaller below the  $\lambda$  point than above. The measurements were transformed to give the radial distribution function  $4\pi r^2[\rho(r)-\rho_0]$  from which was deduced the number of neighbors under the first shell of atoms and the nearest distance of approach of two atoms in the liquid. These lie between 8.3 atoms and 9.3 atoms and 2.35 Å and 2.40 Å, respectively.

### 1. INTRODUCTION

**A** KNOWLEDGE of the atomic distributions, atomic motions and effective potentials in liquids is important in the theory of condensed systems. Information about the atomic distribution in liquids can be obtained from either neutron or x-ray diffraction patterns while information about the atomic motions can be obtained from determinations of the change in energy of inelastically scattered neutrons. Such informations are of particular importance in the case of liquid helium because the details of the  $\lambda$  transition have not been explained and because liquid helium at low temperatures is essentially in its ground state and therefore

the liquid most amenable to theoretical investigations. Both neutrons<sup>1</sup> and x-rays<sup>2-5</sup> have been used to investigate the atomic distribution in liquid helium while the excitation curve has been obtained through measurements of the change in wavelength of neutrons inelastic-

<sup>1</sup> D. G. Hurst and D. G. Henshaw, *Phys. Rev.* **100**, 994 (1955).

<sup>2</sup> W. H. Keesom and K. W. Taconis, *Physica* **5**, 270 (1938).

<sup>3</sup> J. Reekie, *Proc. Cambridge Phil. Soc.* **36**, 236 (1940).

<sup>4</sup> J. Reekie and T. S. Hutchinson, *Phys. Rev.* **92**, 827 (1953); T. S. Hutchinson, C. F. A. Beaumont, and J. Reekie, *Proc. Phys. Soc. (London)* **A66**, 409 (1953); C. F. A. Beaumont and J. Reekie, *Proc. Roy. Soc. (London)* **A228**, 363 (1955).

<sup>5</sup> W. L. Gordon, C. H. Shaw, and J. G. Daunt, *J. Phys. Chem. Solids* **5**, 117 (1958).

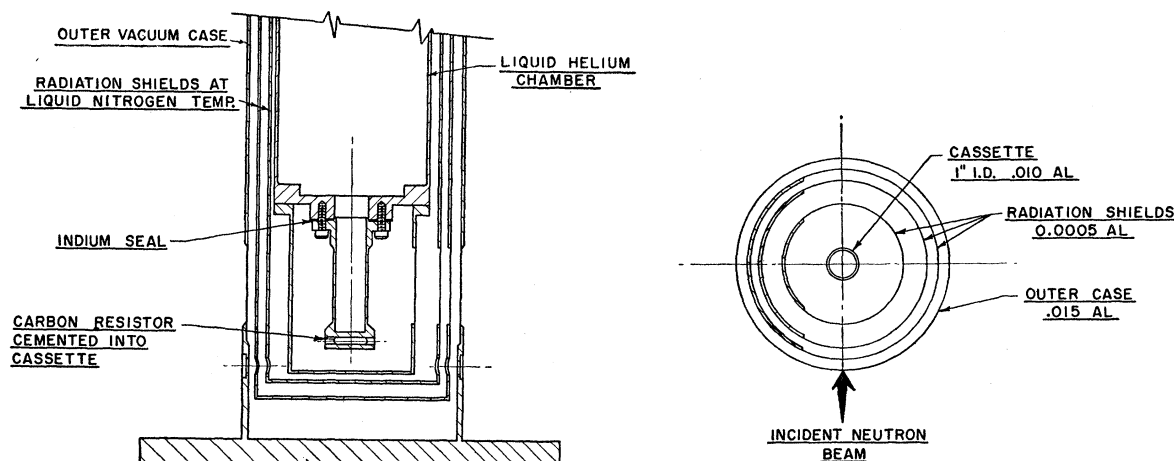


FIG. 1. The scattering chamber used to contain the samples of liquid helium.

cally scattered from liquid helium.<sup>6-8</sup> The measurements<sup>8,9</sup> have shown that there is a marked broadening of the spectrum of the inelastically scattered neutrons associated with the  $\lambda$  transition.

The neutron diffraction measurements<sup>1</sup> suggested a change in distribution of scattered neutrons associated with the  $\lambda$  transition. This change has also been found in later x-ray measurements.<sup>5</sup>

This paper reports remeasurements to higher statistical accuracy of the angular distribution of scattered neutrons at temperature above and below the  $\lambda$  point. The measurements have been transformed to the atomic density distributions in the liquid and analyzed in terms of number of neighbors under the first shell of atoms. The changes in the distributions are discussed in terms of the  $\lambda$  transition.

## 2. APPARATUS

The angular distributions of scattered neutrons were measured using one of the Chalk River Neutron Spectrometers in the arrangement used previously.<sup>10</sup> The cryostat<sup>1</sup> with the scattering chamber modified as shown in Fig. 1, was a 1-in. diameter cassette with walls 0.010 in. thick for a height of  $2\frac{1}{2}$  in. at the level of the neutron beam. The cassette was vacuum sealed to the liquid helium chamber with indium. In this arrangement the liquid used as the refrigerant was also used as the specimen. A carbon resistor,<sup>11</sup> cemented into the base of the cassette, was used as a temperature sensitive element and calibrated against the liquid helium vapor pressure for temperatures down to 1.5°K using the  $T_{55E}$  scale.<sup>12</sup>

<sup>6</sup> H. Palevsky, K. Otnes, K. E. Larsson, R. Pauli, and R. Stedman, Phys. Rev. **112**, 11 (1958).

<sup>7</sup> J. L. Yarnell, G. P. Arnold, P. J. Bendt, and H. C. Kerr, Phys. Rev. **113**, 1379 (1959).

<sup>8</sup> D. G. Henshaw, Phys. Rev. Letters **1**, 127 (1958).

<sup>9</sup> K. Larsson and K. Otnes, Arkiv Fysik **15**, 49 (1959).

<sup>10</sup> D. G. Henshaw, Phys. Rev. **111**, 1470 (1958).

<sup>11</sup> J. R. Clement and E. H. Quinzel, Rev. Sci. Instr. **23**, 213 (1952).

<sup>12</sup> J. R. Clement, J. K. Logan, and J. Gaffney, Phys. Rev. **100**, 743 (1955).

Below 1.5°K the calibration was extrapolated using the semiconductor formula.<sup>11</sup> The temperature of the liquid helium was controlled and recorded by means of its vapor pressure as has been described.<sup>1</sup> It was also recorded by continuously monitoring the resistance of the carbon resistor using an electronic recorder.

## 3. MEASUREMENTS

The angular distributions of 1.064 Å neutrons scattered from liquid helium at the series of temperatures shown in Table I, have been measured at about 210 equally spaced angular points in the angular range 4° to 64° to a statistical accuracy of about  $\pm 2\%$  by recording the number of arm counts for a constant and preset number of monitor counts. The background from the evacuated cassette at temperatures between 4°K and 80°K has been measured at each of the angular points. For angles greater than 10° the background was essentially constant between the lines associated with the fcc structure of the aluminum of the cassette and amounted to about 8% of the total scattering at large angles. Below 10° it rose continuously and became excessive for angles less than 3°. The measured background was corrected for attenuation in the liquid helium using the measured transmission cross section for helium of 0.73 barn<sup>1</sup> before applying it as a correction to the helium curves. The resolution of the instrument, in the region of the main diffraction peak, measured by recording the scattering from powdered KBr and Al was 1.30°.

TABLE I. Liquid helium neutron scattering.

Curve	Liquid temperature (°K)	Helium pressure	Density (g/cc)	Neutron wavelength (Å)
1	1.06	N.V.P.	0.1452	1.06 <sub>4</sub>
2	2.29	N.V.P.	0.1459	1.06 <sub>4</sub>
3	1.06	N.V.P.	0.1452	1.06 <sub>4</sub>
4	2.46	N.V.P.	0.1451	1.06 <sub>4</sub>

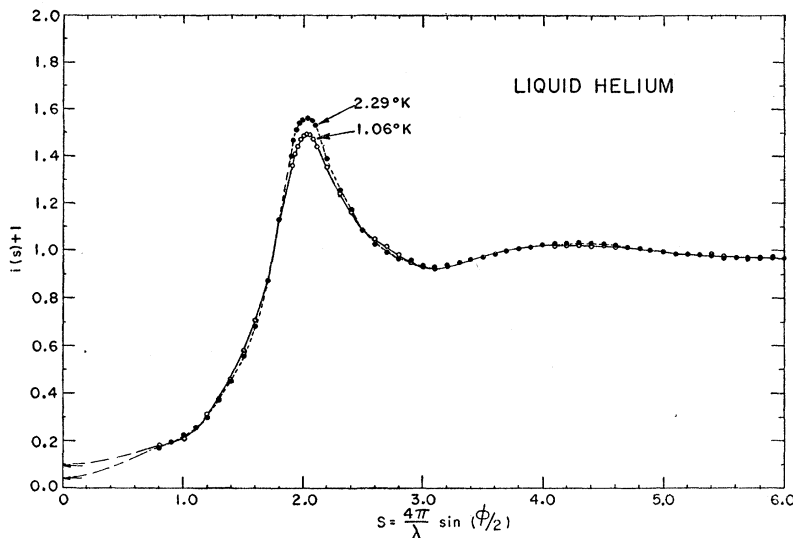


FIG. 2. The liquid structure factor  $i(s)+1$  for liquid helium under its normal vapor pressure at 2.29°K (closed circles) and 1.06°K (open circles) corresponding to densities of 0.1459 g/cc and 0.1452 g/cc, respectively. The effect of the  $\lambda$  transition causes a lowering and broadening of the main maximum.

#### 4. RELATION BETWEEN DENSITY DISTRIBUTIONS AND SCATTERING PATTERNS

The analysis assumes that the scattering is coherent and elastic<sup>1,13</sup> and that the transformation commonly applied to x-ray and neutron scattering is applicable to these measurements. On these assumptions, the measured angular distribution of scattered neutrons may be transformed to the radial distribution function  $4\pi r^2[\rho(r)-\rho_0]$  using the formula<sup>1</sup>

$$4\pi r^2[\rho(r)-\rho_0] = -\frac{2r}{\pi} \int_0^\infty s i(s) \sin(rs) ds, \quad (1)$$

where  $r$ =distance from an atom chosen as center,  $\rho(r)$ =atomic density at a distance  $r$ ,  $\rho_0$ =mean atomic density of the liquid,  $s=(4\pi/\lambda) \sin(\varphi/2)$ ,  $\lambda$ =neutron wavelength,  $\varphi$ =angle of scattering. For liquid helium

$$i(s) = \left( \frac{I_s - \Delta I_{s_{\max}}}{Q_s} - \frac{I_\infty - \Delta I_{s_{\max}}}{Q_{s_{\max}}} \right) / \left( \frac{I_\infty - \Delta I_{s_{\max}}}{Q_{s_{\max}}} \right). \quad (2)$$

$I_s$  is the total scattering<sup>14</sup> and  $Q_s$  is the differential cross section for a free helium atom<sup>15</sup> for the wavelength  $\lambda$  at the corresponding values of the variable  $s$ ,  $\Delta$ =ratio of multiple<sup>16</sup> scattering (assumed isotropic in laboratory

<sup>13</sup> D. G. Henshaw, D. G. Hurst, and N. K. Pope, Phys. Rev. **92**, 1229 (1953).

<sup>14</sup> The total scattering is corrected for background, resolution in the region of the main diffraction peaks, and for multiple scattering solely in the liquid helium.

<sup>15</sup> For a discussion and a theoretical justification of this procedure see N. K. Pope, Report of the Second Informal Symposium on Melting, Diffusion, and Related Topics, Ottawa, October 21-27, 1957 (unpublished).

<sup>16</sup> The multiple scattering included in  $\Delta$  is that arising from neutron scattering both in the liquid helium and walls of the container.

system) to the total scattering at  $s_{\max}$ , the last measured value of  $s$ .

In the analysis of the measurements,  $I_\infty$  is chosen so that

$$-2\pi^2\rho_0 = \int_0^{s_{\max}} s^2 i(s) ds. \quad (3)$$

This ensures that  $\rho(r) \rightarrow 0$  as  $r \rightarrow 0$ . The value of  $\Delta$  was chosen to make the average value of the transform  $r\rho(r)=0$  for spacings out to 2.3 Å the nearest distance of approach of two atoms in the liquid.<sup>17</sup>

#### 5. ANALYSIS

In order to compare the scattering patterns corresponding to Table I, they must be normalized. A suitable function for such a comparison is the liquid structure factor  $i(s)+1$  where  $i(s)$  is defined in Eq. (2). In computing the function  $i(s)$ , the scattering was corrected for background, multiple scattering solely in the liquid helium and for resolution in the region of the main diffraction peaks. The intensities were plotted as a function of  $s$  and the ordinates were read from smooth curves drawn through the points at intervals of  $s=0.1 \text{ Å}^{-1}$  in the range  $0.7 \leq s \leq 6.0 \text{ Å}^{-1}$ . The function  $i(s)$  was then computed using a value of  $I_\infty$  which satisfied Eq. (2) and a value of  $\Delta$  which made the average value of the calculated transforms<sup>18</sup>  $r\rho(r)=0$  for spacings out to 2.3 Å.  $\Delta$  was about 8% of the total scattering at large angles.

The function  $i(s)+1$  is shown in Fig. 2 for the liquid at 2.29°K and 1.06°K. The curve at 2.46°K has not been shown, since it is within experimental error the same as that measured at 2.29°K. The curves of Fig. 2

<sup>17</sup> This method has been used to determine the level of incoherent scattering in other liquids. D. G. Henshaw, Phys. Rev. **105**, 976 (1957); **111**, 1470 (1958).

<sup>18</sup> The Fourier transforms were calculated by Dr. N. K. Pope using the Datatron of the Computation Center, Division of Physics at the Chalk River Laboratories.

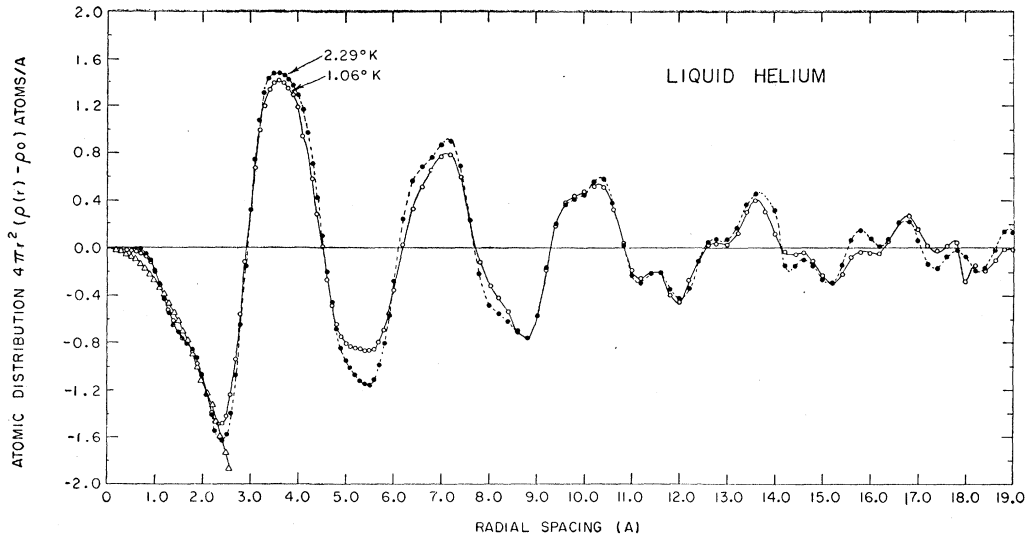


FIG. 3. The radial distribution functions  $4\pi r^2[\rho(r) - \rho_0]$  for each of the curves of Fig. 2. The closed circles and open circles are for the liquid at 2.29°K and 1.06°K, respectively. The curves show that the density fluctuations are less below the  $\lambda$  point than above. The parabolic curve through the triangles is  $-4\pi r^2\rho_0$ , the negative of the mean atomic density.

are similar in form but there are differences in detail. The curves show low scattering at small  $s$  and a peak in the region  $s=2.03 \text{ \AA}^{-1}$  beyond which there is an oscillation about unity with a maximum in the region  $s=4.3 \text{ \AA}^{-1}$ . The curves were extrapolated to 0.04 and 0.095 which represent the level of the zero angle scattering for the liquid at 1.06°K and 2.29°K, respectively, calculated using the compressibility formula<sup>19,20</sup>  $L_0 = nkT\chi_T$  where  $n$  = number of atoms per unit volume,  $k$  = Boltzmann's constant,  $T$  = temperature, and  $\chi_T$  = isothermal compressibility. The height of the first maximum is dependent upon the method of analyzing the curves and in particular upon the choice of  $I_\infty$  which depends mainly on the scattering at large  $s$  because of the  $s^2$  relation in Eq. (3). Because of this, it is estimated that the error in the absolute determination of the peak heights is  $\pm 6\%$  while the relative error between the two curves is  $\pm 2\%$ .

Significant differences between the two curves occur at values of  $s$  less than  $3 \text{ \AA}^{-1}$ . The curves at 2.29°K has a peak which is higher and narrower together with a higher calculated zero angle scattering than the curve at 1.06°K. The ratio of the peak height at 2.29°K to 1.06°K is 1.04, while the ratio of the calculated zero angle scattering is 2.37.

Both curves were transformed to the radial distribution function  $4\pi r^2[\rho(r) - \rho_0]$  in steps of 0.1 Å in the range  $0 \leq r \leq 20.0 \text{ \AA}$ . The results are shown in Fig. 3. For small spacings the functions  $4\pi r^2[\rho(r) - \rho_0]$  oscillate<sup>21</sup> about  $-4\pi r^2\rho_0$  then rise rapidly to a peak at 3.6 Å

beyond which the curves oscillate about zero with an amplitude which decreases with increasing radial spacing. The oscillations in the curve at 2.29°K are somewhat greater than at 1.06°K presumably showing that the spatial order in the liquid at the higher temperature is somewhat greater than at the lower temperature.

To analyze the measurements in terms of the density distribution in the liquid, it is necessary to calculate the function  $4\pi r\rho(r)$ . The changes in this owing to the  $\lambda$  transition are expected to be relatively small since it is the sum of  $4\pi r\rho_0$  and  $4\pi r[\rho(r) - \rho_0]$  which gives the fluctuation of the atomic density about the mean. The changes in the latter, the quantity measured by diffraction measurements, produce relatively small changes in  $4\pi r\rho(r)$  and quantities derived from it. The atomic distribution  $4\pi r\rho(r)$  is shown in Fig. 4 for each of the curves together with  $4\pi r\rho_0$  where  $\rho_0$  corresponds to the liquid density at 2.29°K. The corresponding curve at 1.06°K is only slightly different, lying only 0.7% below the curve at 2.29°K and has not been shown. The atomic distributions  $4\pi r\rho(r)$  for the two temperatures are similar showing oscillations<sup>21</sup> about zero for spacings out to 2.3 Å beyond which there is a maximum at 3.8 Å and oscillations about  $4\pi r\rho_0$  at larger spacings. The ratio of the height of the maximum of the 2.29°K curve to

TABLE II. Analysis of liquid helium atomic distribution functions.

Liquid temperature °K	Radial spacing		Number of nearest neighbors	
	Point where density rises from zero (Å)	Position of maximum in $4\pi r\rho(r)$ (Å)	Peak symmetrical in $4\pi r\rho(r)$ atoms	Peak symmetrical in $4\pi r\rho(r)$ atoms
1.06	2.35	3.80	8.5	9.8
2.29	2.40	3.80	8.5	9.7

<sup>19</sup> F. Zernicke and J. Prins, Z. Physik 41, 184 (1927).

<sup>20</sup> L. Brillouin, Ann. Physik 17, 88 (1922).

<sup>21</sup> As has been discussed,<sup>1,16</sup> these oscillations are most certainly spurious arising from statistical and experimental error and the finite range of  $s$  over which the measurements were made.

the 1.06°K curve is 1.01<sub>8</sub>. At larger  $r$ , the amplitudes of the oscillation of the 2.29°K curve are somewhat greater than those of the 1.06°K curve. Table II gives from an analysis of the curves, the radial spacing where the density rises from zero and the first maximum of  $4\pi r\rho(r)$  together with the number of neighbors under the first shell of atoms which was calculated by two methods. In the first, the number of neighbors under a curve symmetrical in  $4\pi r^2\rho(r)$  about the maximum in  $4\pi r\rho(r)$  was computed while in the second the curve was made symmetrical in  $4\pi r\rho(r)$  about the maximum in  $4\pi r\rho(r)$ . The spacing where the density rises from zero is greater for the curve at 2.29°K than at 1.06°K. The difference, in a direction consistent with the lower order in the liquid at 1.06°K, is smaller than the expected error of the measurements.

## 6. DISCUSSION

The liquid structure factor  $i(s)+1$  has been measured at 1.06°K, 2.29°K, and 2.46°K, the first temperature being below the λ point while the latter two were above. The densities of the liquid are equal at the lowest and highest temperature while at 2.29°K the density of the liquid is higher by 0.7%. There was no difference outside experimental error between the curves at 2.46°K and 2.29°K but the peak of the curve at 1.06°K was lower and broader than the other two. The ratio of the peak height of the curves at 2.29°K to that at 1.06°K is 1.047. This ratio is, within experimental error, the same as the value 1.06 deduced from our earlier neutron measurements<sup>1</sup> for the liquid at 2.25°K and 1.65°K and with the value 1.05 deduced from x-ray measurements<sup>5</sup> for the liquid at 2.4°K and 1.4°K.

The transforms of these measurements show that there is lower spatial order in the liquid below the λ point than above. The major portion of the change occurs in the range 1.65°K to 2.25°K. Inelastic scattering measurements<sup>8</sup> have shown that the atomic motions are more ordered below the λ point than above and that the major portion of the change occurs in the temperature range 1.57°K to 2.08°K. Thus, the liquid below the λ point shows lower spatial order and greater ordering of the atomic motions than above.

The number of neighbors under the first shell of atoms lies between 8.5 atoms and 9.7 atoms, depending upon

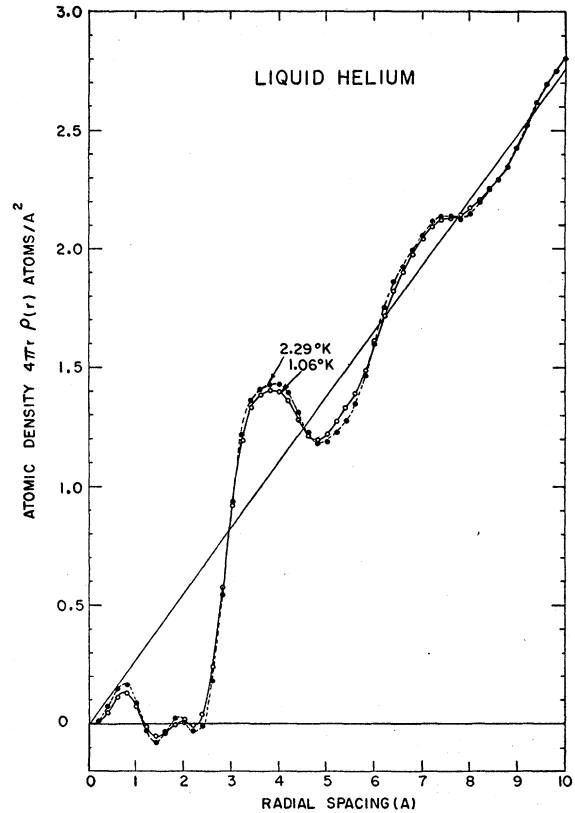


FIG. 4. The atomic density  $4\pi r\rho(r)$  for liquid helium at 2.29°K (closed circles) and 1.06°K (open circles). The straight line is  $4\pi r\rho_0$  the mean atomic density of the liquid at 2.29°K. The mean density for the liquid at 1.06°K is not shown since it differs only slightly from the one shown.

the method of analysis. These values are slightly larger than the value 7.4 and 8.6 found previously<sup>1</sup> but smaller than the number, 10.6 atoms, of the x-ray measurements.<sup>5</sup>

The point where the atomic density  $4\pi r\rho(r)$  deviates from zero is between 2.35 Å and 2.40 Å. This gives the nearest distance of approach of two atoms in the liquid.

## ACKNOWLEDGMENTS

The author wishes to thank Dr. B. N. Brockhouse and Dr. N. K. Pope for helpful discussion and J. R. Freeborn for technical assistance.